Theoretical Analysis of Magnetic Wall Decoupling Method for Radiative Antenna Arrays in Ultrahigh Magnetic Field MRI

XINQIANG YAN,[1,2,3] ZHENTIAN XIE,[4] JAN OLE PEDERSEN,[5] XIAOLIANG ZHANG[4,6]

[1] *State Key Laboratory of Brain and Cognitive Science, Beijing MRI Center for Brain Research, Institute of Biophysics Chinese Academy of Sciences, Beijing 100101, China*
[2] *Key Laboratory of Nuclear Radiation and Nuclear Energy Technology, Institute of High Energy Physics, Chinese Academy of Sciences, Beijing 100049, China*
[3] *Beijing Engineering Research Center of Radiographic Techniques and Equipment, Beijing 100049, China*
[4] *Department of Radiology and Biomedical Imaging, University of California San Francisco, San Francisco, CA 94158*
[5] *Sino-Danish Center for Education and Research, University of Chinese Academy of Sciences, Beijing 100190, China*
[6] *UCSF/UC Berkeley Joint Graduate Group in Bioengineering, San Francisco, CA 94158*

ABSTRACT: Radiative antenna techniques, e.g., dipole and monopole, have been proposed for radiofrequency (RF) coil array designs in ultrahigh field MRI to obtain stronger B_1 field and higher signal-to-noise ratio (SNR) gain in the areas deep inside human head or body. It is known that element decoupling performance is crucial to SNR and parallel imaging ability of array coil and has been a challenging issue in radiative antenna array designs for MR imaging. Magnetic wall or induced current elimination (ICE) technique has proven to be a simple and effective way of achieving sufficient decoupling for radiative array coils experimentally. In this study, this decoupling technique for radiative coil array was analyzed theoretically and verified by a simulation study. The decoupling conditions were derived and obtained from the theory. By applying the predicated decoupling conditions, the isolation of two radiative elements could be improved from about −8 dB to better than −35 dB. The decoupling performance has also been validated by current distribution along the radiative elements and magnetic field profiles in a water phantom. Concepts Magn Reson Part B (Magn Reson Engineering) 45B: 183–190, 2015

KEY WORDS: monopole; dipole; RF coil array; magnetic wall; ICE; decouple; simulation; ultrahigh field; MRI

I. INTRODUCTION

Ultrahigh field (i.e., 7 T and higher) magnetic resonance imaging (MRI), has demonstrated remarking benefits for human imaging, including higher signal-to-noise ratio (SNR), higher spatial resolution, and better image contrast (*1–5*). The high static magnetic fields result in the increase in the Larmor frequency which is usually in radiofrequency (RF) range. At the high frequency of 300 MHz (Larmor frequency of proton at 7 T) and beyond, the wavelength is significantly shortened, especially in high dielectric biological samples, such as human body. The traditional near-field coils, e.g., lumped element *L*/*C* loop resonators and microstrip transmission line resonators (*6,7*), face challenges to provide high SNR gain in the deep areas of human body. To address this problem, far-field coils or radiative antennas, e.g., dipole (*8,9*) and monopole (*10*), have been applied and

Received 18 June 2015; revised 15 August 2015; accepted 22 September 2015

Correspondence to: Xinqiang Yan; E-mail: xinqyan@gmail.com and Xiaoliang Zhang; E-mail: xiaoliang.zhang@ucsf.edu

Concepts in Magnetic Resonance Part B, Vol. 45B(4) 183–190 (2015)

Published online in Wiley Online Library (wileyonlinelibrary.com). DOI: 10.1002/cmr.b.21312

demonstrated stronger B_1 field and higher SNR gain over the conventional near-field coils in the areas deep inside human head and body (*8,10*).

When the monopole or dipole techniques are employed for densely-spaced arrays, e.g., 8-channel or 16-channle arrays for human head imaging, the distance of two adjacent coil elements is smaller than 10 cm (1/10 of the wavelength at 300 MHz). Therefore the close arrangement of coil elements might lead to non-ignorable electromagnetic (EM) coupling, which could decrease the SNR and parallel imaging ability. Several decoupling methods have been successfully applied for traditional loop and microstrip line coil, e.g., element overlapping (*11*), transformers (*12*), and interconnecting *L*/*C* networks (*13*). However, these methods face challenges and not readily feasible for monopole or dipole arrays due to their unique structures. To attain sufficient isolation among the radiative coil elements, the magnetic wall (MW) or induced current elimination (ICE) decoupling technique (*14*) has been proposed and successfully applied for monopole arrays (*15*) and dipole arrays (*16*).

In this study, we aim to theoretically analyze the MW decoupling for radiative coil arrays in ultra-high field MRI and derive the conditions required for achieving sufficient decoupling between radiative elements. Several theoretical methods, including the eigenvalue/eigenvector method, mutual impendence method, and odd/even mode method were employed in the analysis. Decoupling of a coil array is a process of modifying its impedance matrix and reducing all the off-diagonal elements to zero. For eigenvalue/eigenvector method, this can be regarded as a process of equalizing the eigenmode impedances. Mutual impedance method directly rearranges the impedance matrix to a diagonal matrix. Compared with eigenvalue/eigenvector method, mutual impedance method is more straightforward and easier to understand. However, it is limited by the complexity of the impedance matrix and is not suitable for analyzing arrays with high-count channels. Odd–even mode is another widely-used method for analyzing two-element arrays. This analysis assumes that any coupling between two coils can be decomposed into two basic modes, termed even and odd. In the even mode, the currents on both coils have the same direction and amplitude. In the odd mode, the currents on the two coils have the same amplitude but opposite direction. The coupling was totally reduced when the impedances in odd and even modes are the same. To validate the analytical results, transmission coefficient (S_{21}), current distribution, and magnetic field profile of MW decoupled radiative arrays were numerically studied and compared with those of radiative arrays without decoupling treatments.

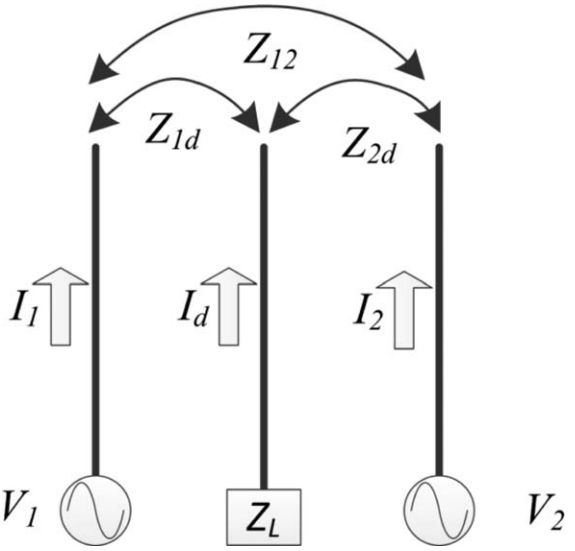

Figure 1 Illustration of two radiative elements and a decoupling element. V_i and I_i are voltage and current across the ports. Z_{ij} are the mutual impedances of the ports. Z_L is the self impendence of the series circuit of the decoupling element.

II. THEORY

Figure 1 shows a coil array consisting of two identical radiative elements and a decoupling element which is placed symmetrically between the two radiative elements. The self and mutual impedances of the two radiative elements (Element 1 and Element 2) and the decoupling element (Element d) are represented by Z_{ii} and Z_{ij}, respectively, where $i \neq j$, $\{i, j\} = 1, 2, d$. V_i and I_i are the voltage and current across the ports of the radiative elements and the decoupling element. The decoupling element includes a decoupling antenna and a series circuit. The self-impedances of the decoupling antenna and the series circuit are $Z_{d',d'}$ and Z_L, respectively.

The current of the decoupling element is totally passive. Therefore, the voltage of the decoupling element is zero and the matrix notation of voltage and current is

$$\begin{bmatrix} Z_{11} & Z_{12} & Z_{1d} \\ Z_{21} & Z_{22} & Z_{2d} \\ Z_{d1} & Z_{d2} & Z_{dd} \end{bmatrix} \begin{bmatrix} I_1 \\ I_2 \\ I_d \end{bmatrix} = \begin{bmatrix} V_1 \\ V_2 \\ 0 \end{bmatrix} \qquad [1]$$

Due to the reciprocity and the symmetry of Element 1 and Element 2, we can get

$$\begin{cases} Z_{d1}=Z_{1d}=Z_{d2}=Z_{2d} \\ Z_{11}=Z_{22} \end{cases} \quad [2]$$

Eigenvalue/Eigenvector Method

In our previous study (*14*), the two coil elements are decoupled when one of the eigenvalues of impedance matrix Z is equal to 0. It is worth noting that although the eigenvalue/eigenvector method is used for reactance matrix X, it could be used for the impedance matrix Z. The requirement of the decoupling element from Ref. (*14*) is

$$Z_{dd}=\frac{z_{1d}^2}{z_{12}} \quad [3]$$

Mutual Impendence Method

From Eqs. [1] and [2], the matrix notation of the voltage and current of Element 1 and Element 2 can simplified as (*17*):

$$\begin{bmatrix} Z_{11}-\frac{z_{1d}^2}{z_{dd}} & Z_{12}-\frac{z_{1d}^2}{z_{dd}} \\ Z_{12}-\frac{z_{1d}^2}{z_{dd}} & Z_{11}-\frac{z_{1d}^2}{z_{dd}} \end{bmatrix} \begin{bmatrix} I_1 \\ I_2 \end{bmatrix} = \begin{bmatrix} V_1 \\ V_2 \end{bmatrix}. \quad [4]$$

The two coil elements were decoupled when the new mutual impendence matrix Z could be simplified as a diagonal matrix. In other words, we require $Z_{12}-\frac{z_{1d}^2}{z_{dd}}=0$. Thus the requirement of the decoupling element is

$$Z_{dd}=\frac{z_{1d}^2}{z_{12}}. \quad [5]$$

Odd/Even Mode Method

For the odd mode, the voltages and currents of the two ports are: $V_1=-V_2=V$; $I_1=-I_2=I$. Thus Eq. [1] can be written as:

$$\begin{bmatrix} Z_{11} & Z_{12} & Z_{1d} \\ Z_{21} & Z_{22} & Z_{2d} \\ Z_{d1} & Z_{d2} & Z_{dd} \end{bmatrix} \begin{bmatrix} I \\ -I \\ I_d \end{bmatrix} = \begin{bmatrix} V \\ -V \\ 0 \end{bmatrix} \quad [6]$$

For the even mode, the voltages and currents of the two ports are: $V_1=V_2=V$; $I_1=I_2=I$. Thus Eq. [1] can be written as:

$$\begin{bmatrix} Z_{11} & Z_{12} & Z_{1d} \\ Z_{21} & Z_{22} & Z_{2d} \\ Z_{d1} & Z_{d2} & Z_{dd} \end{bmatrix} \begin{bmatrix} I \\ I \\ I_d \end{bmatrix} = \begin{bmatrix} V \\ V \\ 0 \end{bmatrix} \quad [7]$$

From Eqs. [6] and [7], the impedances of the odd-mode (referred to as Z_o) and even-mode (referred to as Z_e) can be derived as follows:

$$Z_o=\frac{V}{I}=Z_{11}-Z_{12} \quad [8]$$

$$Z_e=\frac{V}{I}=Z_{11}+Z_{12}-2\frac{z_{1d}^2}{z_{dd}} \quad [9]$$

If $Z_o=Z_e$, the elements are decoupled. Thus, based on Eqs. [8] and [9], the decoupling condition can be derived as

$$Z_{dd}=\frac{z_{1d}^2}{z_{12}} \quad [10]$$

It is clear from Eqs. [3], [5], and [10] that the three theoretical methods gave the same requirement of the decoupling element. Given that the decoupling element includes a decoupling antenna ($Z_{d'd'}$) and a series circuit (Z_L), the required impedance of Z_L:

$$Z_L=\frac{z_{1d}^2}{z_{12}}-Z_{d'd'} \quad [11]$$

III. SIMULATION

A set of EM simulations using a full-wave EM solver (HFSS, ANSYS, Canonsburg, PA) were employed to validate the theoretical analysis described above (*2*). In this article, we only use monopoles as an example to demonstrate this concept. However, the basic principle will work for any coil, e.g., dipole array, since the method only relies on self and mutual impedances. Two monopole elements with and without the decoupling element were modeled in simulation, as shown in Fig. 2(A,B). In the simulations, the length of the decoupling element was chosen the same as the monopole elements. Monopole elements were mounted on a cylindrical former with a diameter of 25 cm. The angle of two monopole elements was varied from 25 to 50 degree with a step of 5 degree [Fig. 2(C)], which means the distance between the two monopoles was varied from 4.3 cm to 10.6 cm. The operating frequency is 297.2 MHz, which corresponds to the Larmor frequency of our 7 T MRI system. A cylindrical water phantom with an outer diameter of 16 cm and a length of 37 cm was placed

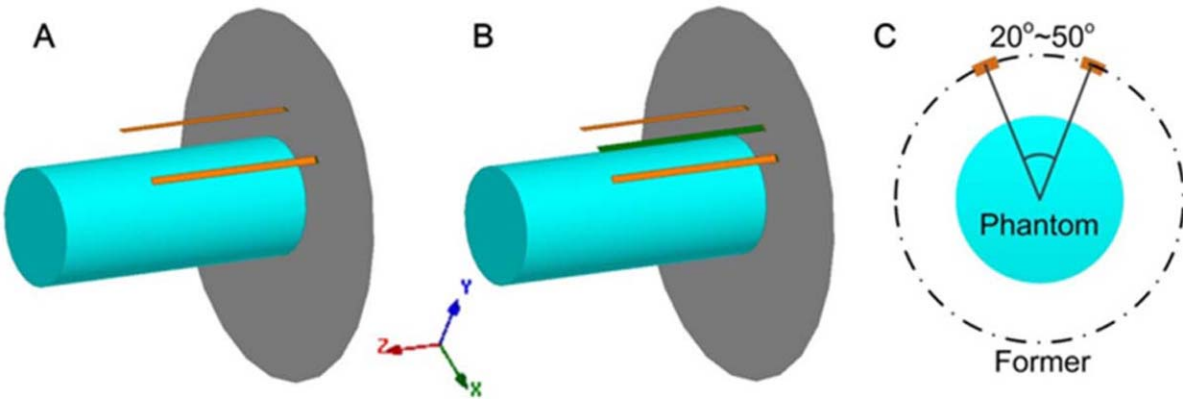

Figure 2 Three-dimensional (3-D) models of 2-channel monopole arrays without (A) and with (B) the decoupling element. C: Cross view of the two monopoles and the water phantom. Monopole elements were mounted on a cylindrical former with a diameter of 25 cm. The angle of two monopole elements was varied from 25 to 50 degree with a step of 5 degree.

4.5 cm below the monopole elements. The EM parameters of the water phantom were set as: conductivity $\sigma = 0.59$ S/m; relative permittivity $\varepsilon_r = 78$. The distance between the boundary and models was larger than $\lambda/2$. Manual mesh was used to accelerate simulation convergence and the convergence condition ΔS was set to 0.002 to achieve more reliable results.

As shown in Fig. 3, the procedure of the validation is:

1. The series circuit of the decoupling element is replaced with a port. Then we get self impedance of the decoupling monopole ($Z_{d'd'}$) and the mutual impedances of monopole-monopole (Z_{12}) and monopole-decoupling element (Z_{1d}).
2. Secondly, the impedance of the serious circuit of decoupling element (Z_L) is obtained by solving Eq. [11].
3. Finally, the equivalent lump component of Z_L is employed in new simulation. S_{21} of the two monopoles, current distribution along the conductors, and the magnetic field on the phantom were obtained and compared with the 2-channel array without decoupling treatments.

IV. RESULTS

Validation of S-Parameter

Z_{12}, Z_{1d}, and $Z_{d'd'}$ obtained from Step 1 of Fig. 3 were listed in Table 1, from the second row to fourth row. The desired Z_L calculated from Eq. [11] was listed in the fifth column. The required resistances of the decoupling elements (referred to as $R(Z_L)$) are assumed to be neglectable because their values are very small. Thus only the imaginary parts of Z_L (referred to as $\mathrm{Im}(Z_L)$) were replaced by lump components (capacitors or inductors), as listed in the sixth column. In order to validate the analysis described above, the equivalent lump components (sixth column of Table 1) were employed in the new simulation (Step 3 of Fig. 3).

Figure 4 shows S_{21} of the two monopole elements with and without decoupling elements. It can be observed that the coupling was reduced from about -8 dB to a sufficiently small value (<-35 dB) when the predicated decoupling elements were employed. This indicates that the theory described above was reliable and can accurately estimate the circuit of the decoupling element. These results have also demonstrated that the assumption of neglectable $R(Z_L)$ is reasonable. Thus only reactance (capacitance or inductance) is needed and no Ohm loss is induced in the decoupling element.

Validation of Current Distribution and *H* Field

Figure 5(A) shows the current density distribution of two coupled monopoles when the left monopole was excited with 1 W while the right monopole was not excited. Due to the mutual coupling, the signal power was obviously coupled to the right monopole, especially when the angle equals to 20 or 25. By using the predicated decoupling elements, however, the coupled signal became neglectable, as shown in Fig. 5(B). This comparison results were in agreement with the S_{21} results as described above. The current directions were indicated by black arrows in Fig. 5(A,B). The current of right monopole using MW decoupling was very small and thus its direction was not shown.

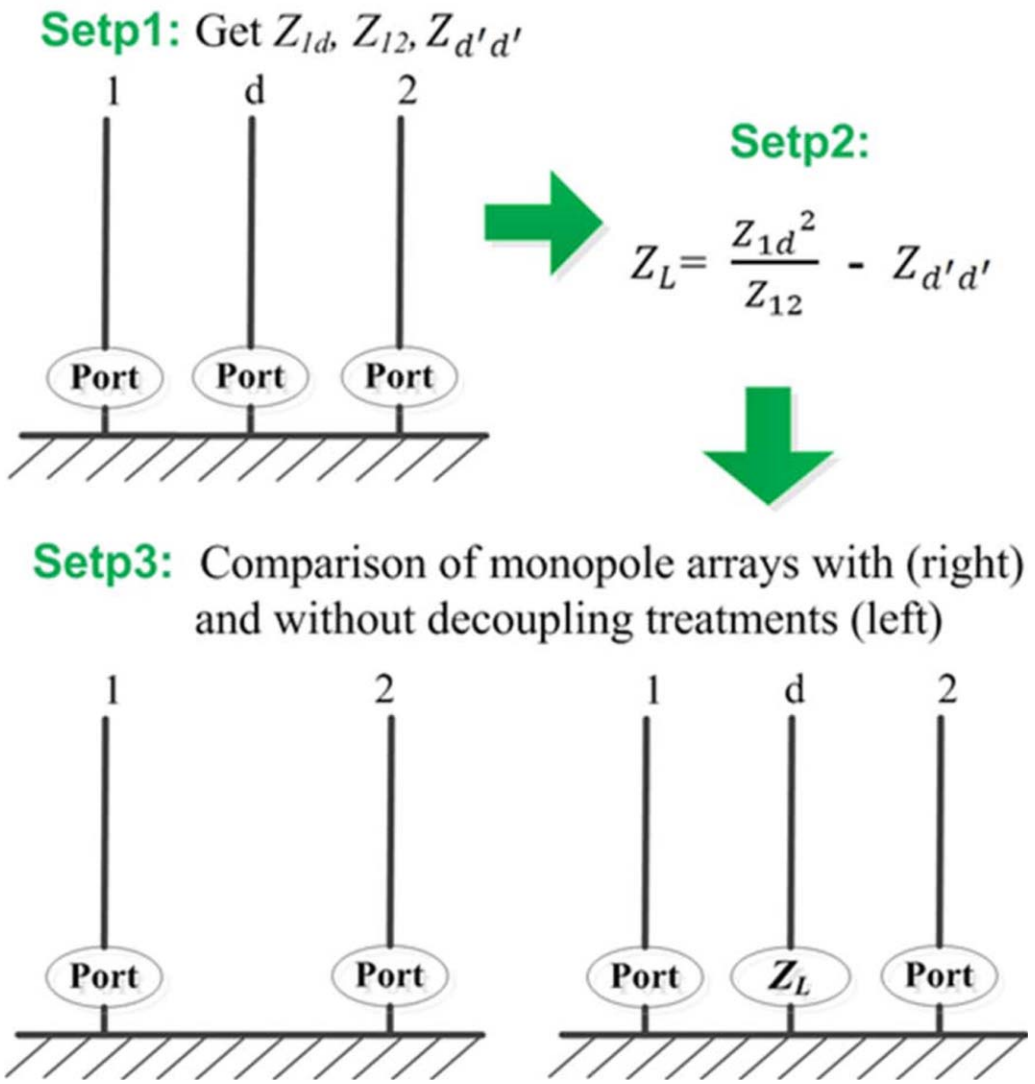

Figure 3 The procedure of validating the theoretical analysis with a EM simulation study.

Figure 5(C,D) shows the normalized *H* field on the water phantom in the transverse plane of monopole arrays without and with MW decoupling method. Clearly, the decoupling elements have shielding effect, making *H* field profiles more independent and weaker at the neighborhood of the two elements. As shown in previous studies (*18*), the shielding effect could benefit the MR imaging in terms of

Table 1 Self and Mutual Impedances of the Monopole Elements and Decoupling Elements

Angle (degree)	Z_{12} (Ω)	Z_{1d} (Ω)	$Z_{d'd'}$(Ω)	Z_L[11] (Ω)	Equivalent of Im (Z_L)
20	$29.637 + j5.438$	$31.769 + j11.39$	$32.9 + j18.673$	$0.145 - j0.2816$	1.9017 nF
25	$27.848 + j2.2095$	$31.087 + j9.3953$	$32.686 + j18.399$	$0.3036 - j0.0403$	13.288 nF
30	$25.8 - j0.63357$	$30.271 + j7.5383$	$32.409 + j18.177$	$0.451 + j0.3192$	0.171 nH
35	$23.551 - j3.0622$	$29.9362 + j5.8832$	$32.071 + j17.979$	$1.9913 + j1.4065$	0.7536 nH
40	$21.215 - j5.0843$	$28.402 + j4.386$	$31.728 + j17.91$	$0.7114 + j1.6080$	0.8615 nH
45	$18.86 - j6.7665$	$27.462 + j2.9963$	$31.507 + j18.248$	$0.7249 + j2.0418$	1.094 nH
50	$16.437 - j8.0404$	$26.338 + j1.689$	$31.061 + j17.975$	$0.7168 + j2.9824$	1.5979 nH

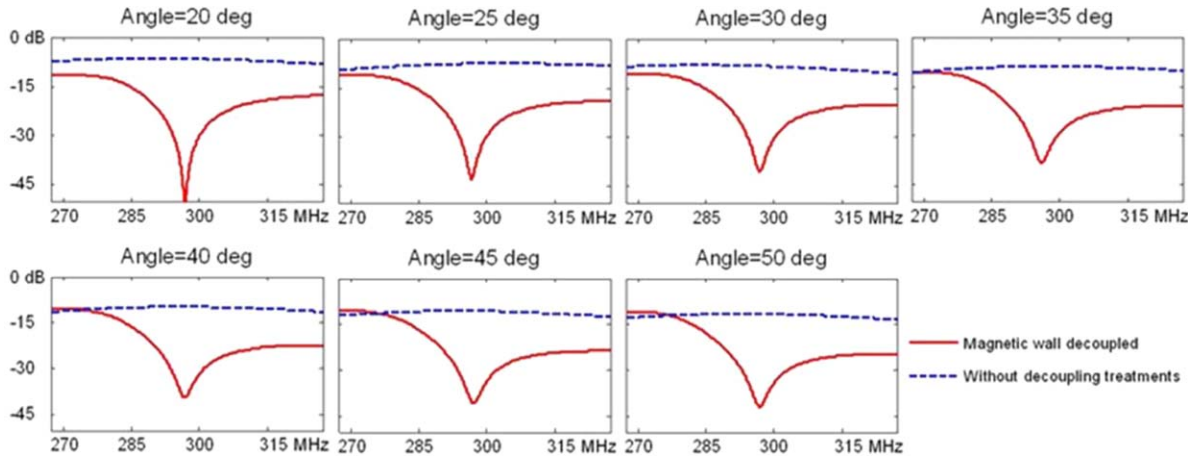

Figure 4 S_{21} plots vs. frequency of the two monopole elements with and without the magnetic wall decoupling method. The series circuits of the decoupling elements used in simulation were calculated from Eq. [11]. It is clear that the strong coupling could be reduced from −6 to −10 dB to a sufficiently small value (better than −35 dB). These results indicate that the theory described above was reliable and it can accurately estimate the requirement of the decoupling element.

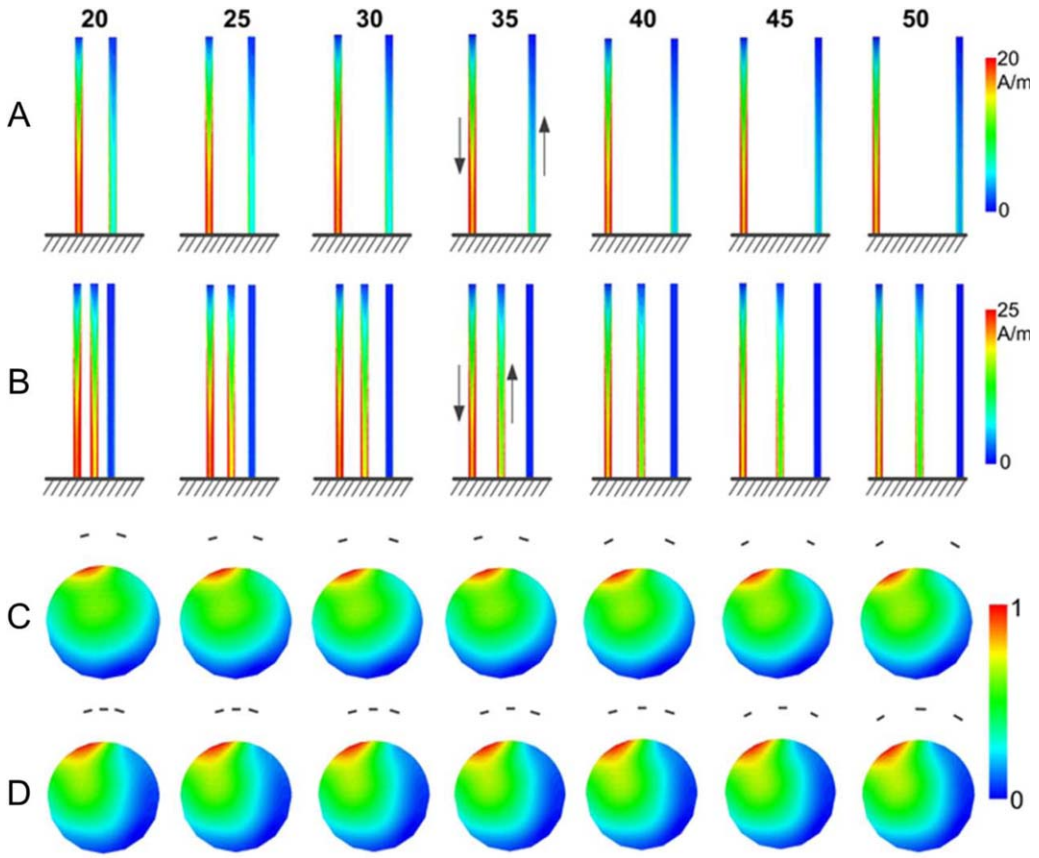

Figure 5 Surface current distributions of monopole arrays and magnetic field profiles on the water phantom. During the simulation, only the left port was excited with 1 W. A: Current distribution of the monopole array without decoupling treatments. B: Current distribution of the MW decoupled monopole array. By using the predicated decoupling element, the coupled current on the right monopoles can be well suppressed. Black arrows in (A) and (B) indicate the current directions along the conductors. C: Magnetic field profile of monopole array without decoupling treatments. D: Magnetic field profile of the MW decoupled monopole array. The magnetic fields near the right monopole become weaker when MW decoupling was employed, which is probably because the decoupling elements act as "magnetic wall" and show shielding effect.

SNR and parallel imaging performance. It can be understood that the shielding effect was generated by the induced current of the decoupling element.

V. DISCUSSIONS AND CONCLUSION

Magnetic wall/ICE decoupling method uses an independent resonator/antenna which has no physical connection to array elements to compensate for the current induced by EM coupling in array elements. In this study, this decoupling method applied for radiative coil array in ultrahigh field MRI was analyzed by using the eigenvalue/eigenvector method, mutual impendence method, and odd/even mode method. The derived conclusions on decoupling conditions from all the three theoretical methods are consistent. These theoretical methods and the decoupling conditions were validated by a set of comparative EM simulations.

The results of numerical analysis on transmission coefficient (S_{21}) between array elements and the induced current distribution have demonstrated that the strong coupling (~ -8 dB) could be reduced to a sufficiently small value (better than -35 dB) by using the decoupling condition obtained from the theoretical analysis. The induced current of the decoupling element caused shielding effect and focused the magnetic field of monopole element (Fig. 5). This focusing generates locally stronger and spatially diverse B_1 fields of antenna array elements, which might be advantageous for MR imaging in terms of SNR and parallel imaging performance.

From Fig. 4, we can find that the decoupling performance still could be better than -30 dB even when the distance between monopoles is only about 5 cm. This indicates that the ICE decoupling method is potential to design radiative coil arrays with high-count channels, e.g., 16 channels. Since the above derivation is purely based on self and mutual impedances, the decoupling element can be arbitrary and need not be of the same type. In other words, the decoupling element could be loop or microstrip line resonators as long as it meets the decoupling condition in Eq. [3].

ACKNOWLEDGMENT

The authors appreciate the invaluable advices from anonymous reviewers of this paper. This study was supported in part by the National Natural Science Foundation of China Grant (51228702), and National Institutes of Health (NIH) R01EB008699.

REFERENCES

1. Yacoub E, Shmuel A, Pfeuffer J, Van de Moortele PF, Adriany G, Andersen P, Vaughan JT, Merkle H, Ugurbil K, Hu XP. 2001. "Imaging brain function in humans at 7 Tesla". Magn Reson Med 45:588–594.
2. Vaughan JT, Garwood M, Collins CM, Liu W, DelaBarre L, Adriany G, Andersen P, Merkle H, Goebel R, Smith MB, Ugurbil K. 2001. "7T vs. 4T: RF power, homogeneity, and signal-to-noise comparison in head images". Magn Reson Med 24:24–30.
3. Lei H, Zhu X, Zhang X, Ugurbil K, Chen W. 2003. "In vivo ^{31}P magnetic resonance spectroscopy of human brain at 7 T". Magn Reson Med 49:199–205.
4. Ibrahim TS, Mitchell C, Schmalbrock P, Lee R, Chakeres DW. 2005. "Electromagnetic perspective on the operation of RF coils at 1.5-11.7 Tesla". Magn Reson Med 54:683–690.
5. Thomas BP, Welch EB, Niederhauser BD, Whetsell WO Jr., Anderson AW, Gore JC, Avison MJ, Creasy JL. 2008. "High-resolution 7T MRI of the human hippocampus in vivo". J Magn Reson Imaging 28:1266–1272.
6. Adriany G, Van de Moortele PF, Wiesinger F, Moeller S, Strupp JP, Andersen P, Snyder C, Zhang X, Chen W, Pruessmann KP, Boesiger P, Vaughan T, Ugurbil K. 2005. "Transmit and receive transmission line arrays for 7 Tesla parallel imaging". Magn Reson Med 53:434–445.
7. Zhang X, Ugurbil K, Chen W. 2001. "Microstrip RF surface coil design for extremely high-field MRI and spectroscopy". Magn Reson Med 46:443–450.
8. Raaijmakers AJ, Ipek O, Klomp DW, Possanzini C, Harvey PR, Lagendijk JJ, van den Berg CA. 2011. "Design of a radiative surface coil array element at 7 T: the single-side adapted dipole antenna". Magn Reson Med 66:1488–1497.
9. Wiggins GC, Zhang B, Lattanzi R, Chen G, Sodickson D. 2012. "The Electric Dipole Array: An Attempt to Match the Ideal Current Pattern for Central SNR at 7 Tesla". In Proceedings 20th Scientific Meeting, International Society for Magnetic Resonance in Medicine. Melbourne, Australia. p 541.
10. Hong SM, Park JH, Woo MK, Kim YB, Cho ZH. 2014. "New design concept of monopole antenna array for UHF 7T MRI". Magn Reson Med. 71:1944–1952.
11. Roemer PB, Edelstein WA, Hayes CE, Souza SP, Mueller OM. 1990. "The NMR phased array". Magn Reson Med 16:192–335.
12. Avdievich NI. 2011. "Transceiver-phased arrays for human brain studies at 7 T". Appl Magn Reson 41:483–506.
13. Wu B, Qu P, Wang C, Yuan J, Shen GX. 2007. "InterconnectingL/C components for decoupling and its application to low-field open MRI array". Concepts Magn Reson B Magn Reson Eng 31:116–126.
14. Li Y, Xie Z, Pang Y, Vigneron D, Zhang X. 2011. "ICE decoupling technique for RF coil array designs". Med Phys 38:4086–4093.

15. Yan X, Zhang X, Wei L, Xue R. 2014. "Magnetic wall decoupling method for monopole coil array in ultrahigh field MRI: a feasibility test". Quant Imaging Med Surg 4:79–86.
16. Yan X, Zhang X, Wei L, Xue R. 2015. "Design and test of magnetic wall decoupling for dipole transmit/receive array for MR imaging at the ultrahigh field of 7T". Appl Magn Reson 46:59–66.
17. Avdievich NI, Pan JW, Hetherington HP. 2013. "Resonant inductive decoupling (RID) for transceiver arrays to compensate for both reactive and resistive components of the mutual impedance". NMR Biomed 26:1547–1554.
18. Yan X, Zhang X, Feng B, Ma C, Wei L, Xue R. 2014. "7T transmit/receive arrays using ICE decoupling for human head MR imaging". IEEE Trans Med Imaging 33:1781–1787.